The spectral variability of the gamma-ray emission from Geminga and VELA and its implications

Grenier, I.A.; Hermsen, W.; Henriksen, R.N.

Astron. Astrophys. 269, 209–218 (1993)

ASTRONOMY AND ASTROPHYSICS

The spectral variability of the γ-ray emission from Geminga and Vela and its implications

I. A. Grenier[1,2], W. Hermsen[3], and R. N. Henriksen[4]

[1] EUROPA, Université de Paris Denis Diderot, Observatoire de Paris, France
[2] Service d'Astrophysique, Centre d'Etudes de Saclay, F-91191 Gif/Yvette, France
[3] Laboratory for Space Research Leiden, Leiden, The Netherlands
[4] Queen's University, Kingston, Canada

Received September 15, accepted October 5, 1992

Abstract. The γ-ray emissions from Geminga and from the Interpeak 1 component of the Vela pulsar were analysed in order to compare their spectral properties between 50 MeV and 5 GeV and to study their variability between 1975 and 1982 using the COS-B data. The stability of both sources above about 200 and 300 MeV, respectively, retaining an $E^{-2.0 \pm 0.1}$ spectrum of constant intensity over these years, is remarkable. At lower energies, however, their spectral distribution has been found to be variable at the 4 σ and 5 σ level, respectively. Both sources exhibit a high state, characterized by a power-law spectrum of index close to -2 that extends down to 50 MeV. In a low state, their soft radiation below a few hundred MeV is largely suppressed for long periods. The induced spectral breaks in the low states were detected at 5 σ and 4 σ significance, respectively.

The parallel behaviour of the two sources hints at a common origin of their very hard γ radiation and of its long term variability. It may find its roots in the properties of curvature radiation or very small pitch-angle synchrotron radiation, as discussed here.

Key words: pulsars: individuals: PSR0833+45, 2CG195+04 – pulsars: general – gamma rays: observations – radiation mechanisms: cyclotron and synchrotron

1. Introduction

The second brightest source in the GeV sky, Geminga or 2CG195+04, eluded a clear identification for 20 years. An association with the X-ray source 1E0630+178 and a blue 25th magnitude star (G") was first proposed because of their unusual combination of spectral properties and the implied L_γ/L_X and L_X/L_V ratios of order 1000 and 1800, respectively, that recalled the characteristics of the young Vela pulsar (Bignami et al. 1988; Halpern & Tytler 1988). The comparison with Vela favoured the idea of Geminga being a pulsar which was later substantiated by the similarity we found in the details of their γ radiation (Grenier et al. 1991). At the end of the present work, ROSAT X-ray data from 1E0630+178 and EGRET high-energy γ-ray data from Geminga revealed that the two sources are indeed one and the same: a pulsar with a period of 237 ms (Halpern & Holt 1992; Bertsch et al. 1992)... and we were delighted to update our paper! This important discovery brings us an additional example of a high-energy γ-ray pulsar to unveil detailed aspects of pulsar emission. In fact, the analysis of data from the Compton Gamma-Ray Observatory has recently increased the number of firm γ-ray pulsars from two (Crab & Vela) to five, including the 102-ms pulsar PSR1706-44 identified by EGRET with the COS-B source 2CG342-02 (Swanenburg et al. 1981; Kniffen et al. 1992), and the 150-ms pulsar PSR1509-58 detected by BATSE up to possibly a few MeV (Wilson et al. 1992).

In the X rays, the soft, broad pulse of emission from 1E0630+178 recalls the weakly modulated thermal emission that arises from Vela, possibly from the surface of the neutron star (Ögelman et al. 1991). The lack of interstellar absorption towards 1E0630+178 yields an upper limit of 500 pc to the distance of Geminga (Halpern & Holt 1992). Above 100 MeV, the Geminga and Vela light curves show common features: two narrow peaks bracketing an interpeak region of emission (Bertsch et al. 1992; Bignami & Caraveo 1992; Hermsen et al. 1992). But, the phase separation of 0.5 $\pm$ 0.03 between the peaks probably indicates a different location of the γ-ray emitting site in the magnetosphere of Geminga compared to that of Crab & Vela where the phase separation is only 0.42.

In order to present another similarity between Vela and Geminga, linked to their variable aspect in γ rays, this article gathers the spectral information that was obtained between 50 MeV and 5 GeV, over seven years, from the repeated COS-B observations of Geminga and of the Interpeak 1 component of the Vela pulsed emission. This component was selected from the five independent phase intervals of the Vela light curve because it showed signs of a spectral variability analogous to what

Send offprint requests to: I.A. Grenier, DAPNIA/SAp, C.E. Saclay, 91191 Gif/Yvette Cedex, France

Table 1. Characteristics of Geminga and Vela observations

Observing period	Pointing direction (l,b)	Source aspect angle	Start, end dates (d/m/y)
	Geminga:		
0	183°.9, -6°.1	15°	17/08/75
			17/09/75
14	195°.2, +4°.2	0°	30/09/76
			01/11/76
39	190°.2, -0°.3	7°	22/02/79
			02/04/79
54	188°.4, -2°.5	9°	04/09/80
			16/10/80
64	190°.1, +0°.2	6°	18/02/82
			25/04/82
	Vela:		
2	263°.5, -3°.4	1°	20/10/75
			07/11/75
3	262°.7, +3°.4	6°	08/11/75
			28/11/75
45	263°.0, +3°.9	7°	10/10/79
			15/11/79

was found for Geminga (Grenier et al. 1988, alias GHC 1988 later on; Grenier et al. 1991). Not knowing the Geminga period at that time, no phase selection was applied. A similar spectral analysis as a function of phase is now under way and will be published separately with an accurate timing analysis of the γ-ray pulsation and a study of the morphology of the light curve. An average spectrum of Geminga had been derived in 1981 by Masnou et al., but the present study includes all available observations up to 1982 and it focuses on the spectral evolution of the source with time and on the existence of a spectral break around a few hundred MeV.

2. Data and analysis

COS-B operated in the 50-5000 MeV range. It was pointed near Geminga five times between 1975 and 1982 for durations of one to two months. The observing periods are listed in Table 1. Five COS-B observations of Vela have been previously analysed (GHC 1988). The three listed in Table 1 were selected for a more detailed analysis to compare the behaviour of Vela to that of Geminga. The collected photons and the related instrumental characteristics, such as the sensitive area, point-spread-function, and energy resolution, have been retrieved from the Final COS-B Database (Mayer-Haßelwander 1985). The telescope sensitivity decreased during its lifetime. The relative efficiency for each observing period has been taken from the study of overlapping observations along the Galactic plane (Strong et al. 1987).

The spectral deconvolution of the source radiation used the maximum-likelihood method developed to describe the Vela pulsar emission (GHC 1988). The procedure treats the photons individually by computing the probability density function of detecting a photon at a measured energy and position, coming from a given source model. The photons are not binned spatially, nor in energy, to take full account of the modest energy and spatial resolutions of the COS-B detector. The likelihood of a model is simply the product of the probabilities of detecting the independent events actually recorded by COS-B. As a boundary condition, the total number of photons detectable from a model was assumed to equal the total number of photons collected within the entire COS-B field-of-view and energy band.

In the case of the Geminga observations, the model includes four different sources to describe the bulk of the γ rays detected in the large telescope field-of-view:

1. a constant and isotropic instrumental background of free intensity and spectral index.
2. the steady diffuse Galactic emission in the whole field-of-view. Its spatial structure can be traced by HI and CO maps of the region (see Strong et al. 1988 and references therein). Its intensity and spectral index were treated as free parameters.
3. the point-sources of the Crab pulsar and its nebula, at their radio position: their stable power-law spectra have been directly taken from the analysis of Clear et al. (1988).
4. the point-source Geminga at l= 195°.1 and b= 4°.2 for which we examined different spectral distributions.

To study the Vela Interpeak 1 emission, the model includes the instrumental and Galactic background emissions and a point-source at the radio position of the Vela pulsar. Only photons in the 0.15 - 0.33 phase interval were selected (see GHC 1988).

As a first step, single-power-law spectra, covering the whole 50-5000 MeV interval, were compared to the data of each observation independently. The spectra from the instrumental and Galactic backgrounds, and from the relevant source (Geminga or Vela) were fitted simultaneously. This provides a useful check on instrumental variations in sensitivity and energy response over the years since they should show up similarly in the behaviour of the background and source spectra.

The analysis has been applied then to test the existence of a low-energy spectral break. Two-power-law distributions, covering the whole 50-5000 MeV range with two independent indices, γ_L and γ_H, below and above a given energy threshold, were fitted to the source emission of each observation. Various break energies, ranging from 100 MeV to 380 MeV, were examined. The introduction of a free parameter in the likelihood analysis for the break energy would require too much CPU-time to be practical. To allow for smoothly curved distributions at low energy, a "parabolic+power-law"shape has also been tested by coupling an $E^{A.\log E} . E^B$ spectrum below a given energy threshold to an E^{-2} power law above that threshold. The choice of a -2 index corresponds to the stable, average value of γ_H found at high energy for the two-power-law fits. For Vela, this index further characterizes the pulsed emission, at high energy, in all different parts of the light curve over the years (GHC 1988). The "parabolic+power-law"representation has no physical ba-

Table 2. Single power-law spectra fitted to the 50–5000 MeV emission from Geminga for the separate observations, the average of all five periods (<>), and the low-activity average (low <>) of all periods but 14

period	$\gamma\ cm^{-2}\ s^{-1}\ MeV^{-1}$
0	$(2.6\ ^{+3.5}_{-1.5})\ 10^{-5}\ E_{MeV}^{-1.50\pm0.15}$
14	$(4.7\ ^{+3.0}_{-2.0})\ 10^{-4}\ E_{MeV}^{-2.02\pm0.10}$
39	$(1.2\ ^{+0.8}_{-0.5})\ 10^{-5}\ E_{MeV}^{-1.77\pm0.10}$
54	$(1.4\ ^{+1.3}_{-0.7})\ 10^{-5}\ E_{MeV}^{-1.80\pm0.12}$
64	$(2.1\ ^{+1.4}_{-0.9})\ 10^{-5}\ E_{MeV}^{-1.87\pm0.10}$
<>	$(1.7\ ^{+0.5}_{-0.4})\ 10^{-4}\ E_{MeV}^{-1.84\pm0.05}$
low <>	$(9.0\ ^{+3.6}_{-2.5})\ 10^{-5}\ E_{MeV}^{-1.77\pm0.06}$

Table 3. Spectral indices of the Geminga emission for double-power-law spectra between 50 MeV and 5 GeV, obtained for the separate observations, the average of all five periods (<>), and the low-activity average (low <>) of all periods but 14. The significance of a spectral break is measured from the maximum-likelihood values of the single and double power-law fits. An asterisk marks the best fit.

Period	Break energy (MeV)	Low-energy index γ_L	High-energy index γ_H	Break confi--dence
0	140 *	$> 0.\ (1\ \sigma)$	$-1.8\ \pm0.2$	$2.2\ \sigma$
	200	$+0.3\ ^{+1.2}_{-1.1}$	$-1.8\ \pm0.2$	$2.0\ \sigma$
	290	-0.60 ± 0.55	-1.95 ± 0.30	$1.9\ \sigma$
14	100	$-2.7\ ^{+1.3}_{-0.8}$	-1.98 ± 0.10	~0
	140	-2.15 ± 0.55	-1.98 ± 0.13	~0
	200	$-2.0\ ^{+0.3}_{-0.4}$	-2.00 ± 0.15	~0
	290	$-2.0\ \pm0.2$	-2.01 ± 0.18	~0
39	140	$> +6.\ (1\ \sigma)$	-2.25 ± 0.18	$4.1\ \sigma$
	200 *	$+1.3\ ^{+1.7}_{-0.9}$	-2.40 ± 0.20	$4.5\ \sigma$
	290	-0.45 ± 0.45	-2.55 ± 0.30	$4.1\ \sigma$
	380	$-1.0\ \pm0.3$	$-2.6\ \pm0.3$	$3.5\ \sigma$
54	140	$+1.5\ ^{+10.0}_{-2.1}$	-2.08 ± 0.20	$2.1\ \sigma$
	200 *	$-0.2\ ^{+1.2}_{-0.8}$	-2.23 ± 0.24	$2.4\ \sigma$
	290	$-1.0\ \pm0.5$	$-2.3\ \pm0.30$	$2.3\ \sigma$
64	100 *	$> +0.5\ (1\ \sigma)$	-2.05 ± 0.15	$2.1\ \sigma$
	140	$-0.9\ \pm0.8$	-2.00 ± 0.15	$1.3\ \sigma$
	200	$-1.7\ \pm0.4$	-1.93 ± 0.15	$0.4\ \sigma$
	290	-1.80 ± 0.25	-1.92 ± 0.18	
<>	140 *	$-0.4\ \pm0.6$	-2.02 ± 0.07	$4.7\ \sigma$
	200	$-1.1\ \pm0.3$	-2.07 ± 0.09	$4.5\ \sigma$
	290	-1.45 ± 0.15	-2.12 ± 0.10	$4.1\ \sigma$
low <>	140 *	$+1.4\ \pm1.0$	-2.04 ± 0.08	$5.2\ \sigma$
	200	$-0.5\ \pm0.35$	-2.10 ± 0.11	$4.9\ \sigma$
	290	-1.10 ± 0.22	-2.15 ± 0.15	$4.5\ \sigma$

sis, nor does the two-power-law function. But, having no a-priori knowledge of the radiation process, these representations conveniently circumscribe the actual spectral shape. Introducing a second break at GeV energies failed because the scarce photons arising from Vela or Geminga above a few GeV could not constrain the fits.

Table 4. Spectral indices of the Vela Interpeak 1 emission for double-power-law spectra between 50 MeV and 5 GeV, obtained for the separate observations, the average of all five periods (<>), and the low-activity average (low <>) of periods 2 and 45. The significance of a spectral break is measured from the maximum-likelihood values of the single and double power-law fits. An asterisk marks the best fit.

Period	Break energy (MeV)	Low-energy index γ_L	High-energy index γ_H	Break confi--dence
2	140	$+2.5\ ^{+2.0}_{-2.8}$	-1.85 ± 0.17	$1.7\ \sigma$
	200	$0.0\ ^{+1.3}_{-0.9}$	-1.95 ± 0.19	$2.0\ \sigma$
	290 *	$-0.6\ \pm0.55$	-2.10 ± 0.23	$2.3\ \sigma$
	380	-0.95 ± 0.35	-2.18 ± 0.28	$2.1\ \sigma$
3	140	$-1.6\ ^{+0.7}_{-0.6}$	-2.05 ± 0.15	$0.5\ \sigma$
	200 *	-1.63 ± 0.41	-2.13 ± 0.22	$0.9\ \sigma$
	290	-1.77 ± 0.27	-2.16 ± 0.24	$0.8\ \sigma$
	380	-1.85 ± 0.22	-2.17 ± 0.30	$0.6\ \sigma$
45	200	$> +1.0\ (1\ \sigma)$	-2.25 ± 0.26	$3.5\ \sigma$
	290 *	$+0.3\ \pm0.8$	$-2.4\ \pm0.3$	$3.6\ \sigma$
	380	$-0.4\ \pm0.5$	$-2.6\ \pm0.4$	$3.4\ \sigma$
low <>	200	$+1.0\ ^{+1.3}_{-1.0}$	-2.05 ± 0.15	$3.9\ \sigma$
	290 *	-0.25 ± 0.43	-2.23 ± 0.18	$4.2\ \sigma$
	380	-0.72 ± 0.28	-2.36 ± 0.23	$4.0\ \sigma$

3. Results

The results of the various single and double power-law fits to the data of the separate observations, or of combinations of observations, are summarized for Geminga in Tables 2 and 3, and for Vela Interpeak 1 in Table 4. The increase in likelihood obtained between the single and double power-law fits measures the improvement in the quality of the fit caused by the introduction of a spectral break. The corresponding statistical significance of the break is given in Tables 3 and 4.

To study the time-averaged behaviour of Geminga between 1975 and 1982, all five observations have been combined. The resulting best single-power-law fit is for $50 \leq E \leq 5000$ MeV:

$$S(E) = (1.7\ ^{+0.5}_{-0.4})\ 10^{-4}\ E_{MeV}^{-1.84\pm0.05}\ \gamma\ cm^{-2}\ s^{-1}\ MeV^{-1} \quad (1)$$

The binned spectrum measured by Masnou et al. (1981) for the sum of observations 0, 14, 39, and 54 led to an $E^{-1.8}$ spectrum between 100 and 3200 MeV that possibly ($2\ \sigma$) flattened and steepened below and above these limits. Hence, two-power-law spectra with break energies of 140, 200 and 290 MeV were tested. According to the maximal likelihood values reached in the various cases, the fit improves when decreasing the energy

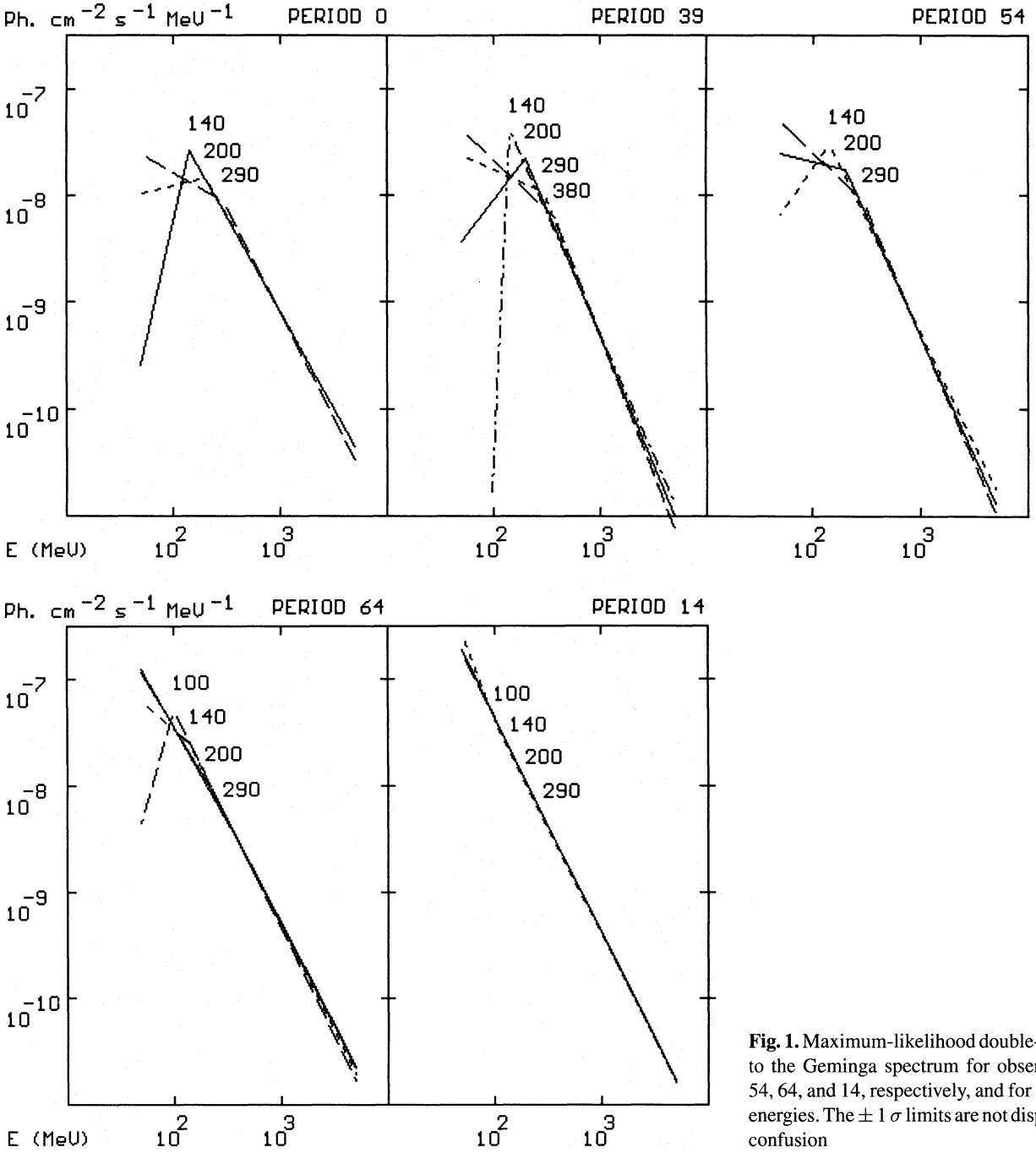

Fig. 1. Maximum-likelihood double-power-law fits to the Geminga spectrum for observations 0, 39, 54, 64, and 14, respectively, and for different break energies. The $\pm 1\,\sigma$ limits are not displayed to avoid confusion

of the break. So, the time-averaged spectrum of Geminga is best represented by the following distribution:

for $50 \leq E \leq 140$ MeV:
$S(E) = (1.6\ ^{+30.3}_{-1.5})\ 10^{-7}\ E_{MeV}^{-0.4 \pm 0.6}$ $\gamma\ cm^{-2}\ s^{-1}\ MeV^{-1}$ (2a)

for $140 \leq E \leq 5000$ MeV:
$S(E) = (6.2\ ^{+2.8}_{-2.2})\ 10^{-4}\ E_{MeV}^{-2.02 \pm 0.07}$ $\gamma\ cm^{-2}\ s^{-1}\ MeV^{-1}$ (2b)

It fully agrees with the Masnou et al. (1981) binned spectrum. The increase in likelihood measured between the single (1) and double (2) power-law fits clearly supports the existence of a break at low energy at a significance level well over $4\,\sigma$ (Table 3). The break does not seem to occur at a precise energy, but the flattening becomes gradually more pronounced when lowering the break position in energy. The photon statistics were insufficient to test a break energy lower than 140 MeV.

To study the spectral evolution of Geminga with time, the likelihood analysis was applied to each observation independently. The maximum-likelihood two-power-law fits found for different break energies are displayed on Fig. 1 for the five observations. A pronounced break is detected for each observation except for period 14. For the latter, break energies of 100, 140, 200 and 290 MeV have been tested, but all fits reach a

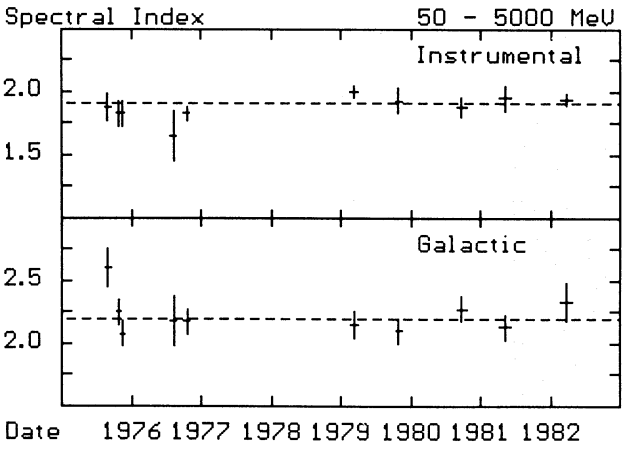

Fig. 2. Spectral indices of the instrumental and Galactic background emissions present in the COS-B field-of-view during Vela and Geminga observations (periods 2, 3, 12, 14, 39, 45, 54, 59, and 64)

remarkably constant likelihood value equal to that of the single-power-law fit. So, the Geminga spectrum during period 14 is best represented by the following power law for 50 $\leq$E$\leq$ 5000 MeV:

$$S(E)= (4.7\ ^{+3.0}_{-2.0})\ 10^{-4}\ E_{MeV}^{-2.02\pm0.10} \quad \gamma\ cm^{-2}\ s^{-1}\ MeV^{-1} \quad (3)$$

It coincides at high energy with the time-averaged spectrum (2). Below 200 MeV, however, the discrepancy between the source distributions (2) and (3) reveals a significant spectral variability (3.9 to 4.3 σ according to the choice of break energy in the average distribution). Furthermore, an instrumental cause can be excluded. The energy response of the COS-B detector has proved to be rather stable during its lifetime (Strong et al. 1987). This stability has been independently checked in the present analysis and in the former spectral study of the Vela pulsar emission (GHC 1988). The simultaneous determination of the spectral indices of the underlying instrumental and Galactic emissions indicates no change in the instrument response with time and energy (Fig. 2). The Crab pulsar also lay in the COS-B field-of-view during the Geminga observations and it showed no signs of spectral variability (Clear et al. 1988, and references therein). Finally, during all Vela observations, the pulsed emission from the first peak remained constant in intensity and spectral index (GHC 1988).

The determination of an average spectral index for the Galactic diffuse emission is by itself an interesting result. The average index for the about one steradian field-of-view around the Vela and Galactic anticenter directions was found to be close to 2.2. This is the first derivation of this index taking into account the full COS-B detector response. It is roughly consistent with the work by Bloemen (1987) and Bloemen et al. (1988) who studied this parameter for the inner and outer Galaxy and as a function of Galactic latitude. The slight difference may arise from the full spectral deconvolution applied here.

A flattening of the spectrum below 100 - 300 MeV marks the four periods of "low activity"of Geminga. To evaluate the hardness of the radiation in this state, the "low-activity"average spectrum has been computed for break energies of 140, 200 and 290 MeV from the combination of periods 0, 39, 54 and 64. The maximum-likelihood fits are displayed on Fig. 3a. Having removed the data from the discrepant period 14, the significance of a spectral break in the "low-activity"state rises to $\sim$5 σ (Table 3) and the significance of a spectral variability between period 14 and the low-activity state reaches 5.2 to 5.3 σ for the different choices of break energy. When lowering the energy of the break, the gradual flattening of the spectrum and the increasing significance of a break strongly suggest that the real source spectrum is smoothly curved at lower energies. This shape has been circumscribed by testing a parabolic distribution (on a log-log scale) below 380 MeV, coupled to an E^{-2} power-law above the threshold that is representative of the stable, average spectrum at high energies. The maximum-likelihood parabolic fit and its 1, 2, and 3 σ confidence regions are presented on Fig. 3b.

In the Vela pulsar γ-ray light curve, five discrete components were identified because of their different spectral distributions below 300 MeV and of their different evolutions on a timescale of weeks to months (GHC 1988). Among them, the Interpeak 1 emission, appearing just after the first main peak, behaved much like Geminga and therefore was chosen for further investigations. Break energies other than 300 MeV have been tested to show the severe depletion of soft emission at certain times below 200 MeV. COS-B observing periods 2 and 45 were selected as examples of the Interpeak 1 source in a low state and period 3 to illustrate the source behaviour in a high state. The results of single-power-law fits to the Interpeak 1 emission can be found in GHC 1988. Figure 4 and Table 4 of the present paper summarize the results of double-power-law fits for different break positions in energy and the related statistical significance of a spectral break. As expected, a pronounced break at low energy is seen in periods 2 and 45, but not during period 3.

To show the hardness of the Interpeak 1 emission in a low state of activity, periods 2 and 45 were merged and break energies of 200, 290, and 380 MeV were considered. The corresponding best two-power-law fits are displayed on Fig. 5a. The comparison of the likelihood values reached for the single and double power-law fits clearly supports a flattening of the low-activity average spectrum at low energy, at a statistical level of about 4 σ (Table 4). The result of a parabolic + power-law fit and its $\pm1\rho$ confidence regions are presented in Fig. 5b. The fit is not so well constrained as in the case of Geminga because of the lack of soft source photons.

In a high state, the double-power-law fits to the data of period 3 seem to favour a low-energy index γ_L of absolute value slightly lower than the 2.00 ± 0.11 value obtained for the single-power-law fit (Table 4 and GHC 1988). But, the corresponding slight increase in likelihood does not firmly establish the presence of a break in the spectrum. From a statistical point-of-view, the high-state spectral distribution of the Interpeak 1 emission, integrated between 0.15 and 0.33 in phase, is well represented by the power law for 50 $\leq$E$\leq$ 5000 MeV:

$$S(E)= (4.2\ ^{+3.2}_{-1.9})\ 10^{-4}\ E_{MeV}^{-2.00\pm0.11} \quad \gamma\ cm^{-2}\ s^{-1}\ MeV^{-1} \quad (4)$$

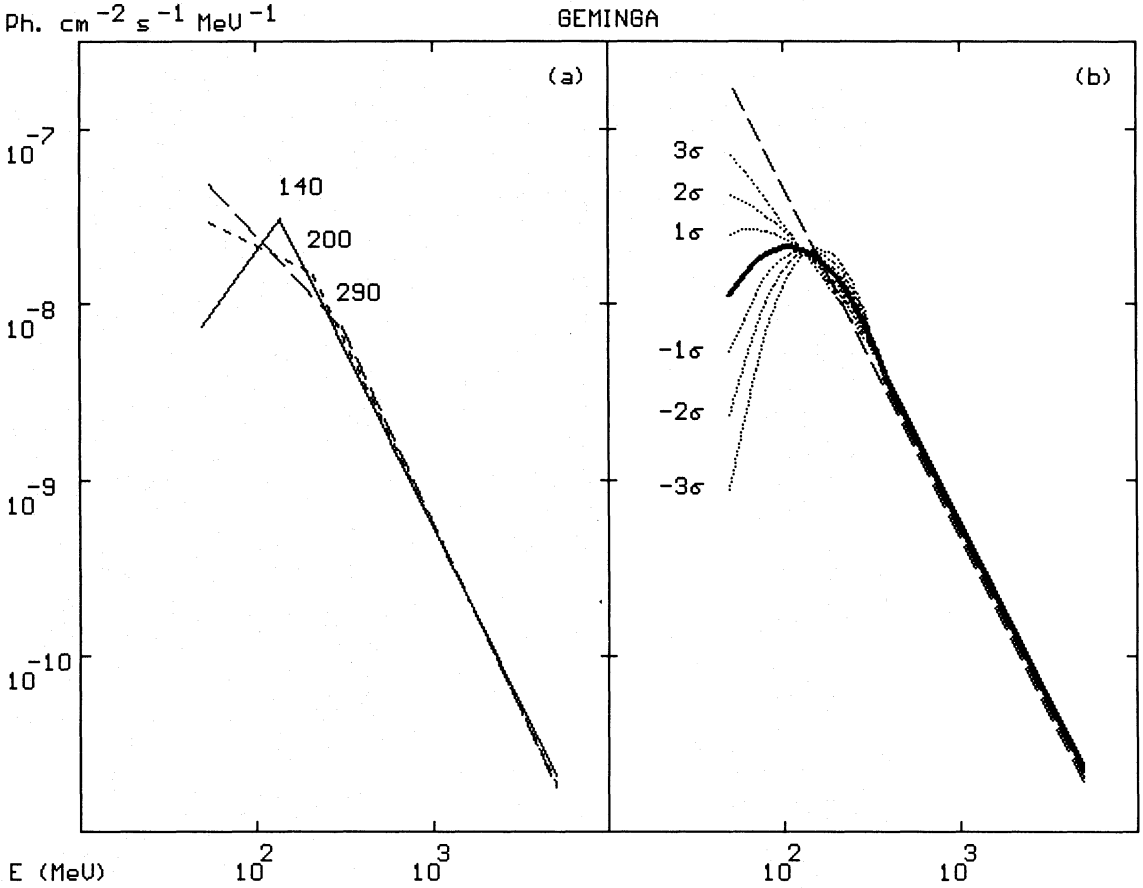

Fig. 3a and b. Maximum-likelihood fit to the Geminga emission in a low state of activity from the combinations of periods 0, 39, 54, and 64: **a** double-power-law fits for break energies at 140, 200 and 290 MeV. Their $\pm$ 1 σ limits are not drawn to avoid confusion. **b** parabolic fit coupled to an E^{-2} spectrum above 380 MeV (thick line) and its $\pm$ 1, 2, and 3 σ confidence regions (dotted lines). The dashed line shows the high-state spectrum obtained during period 14

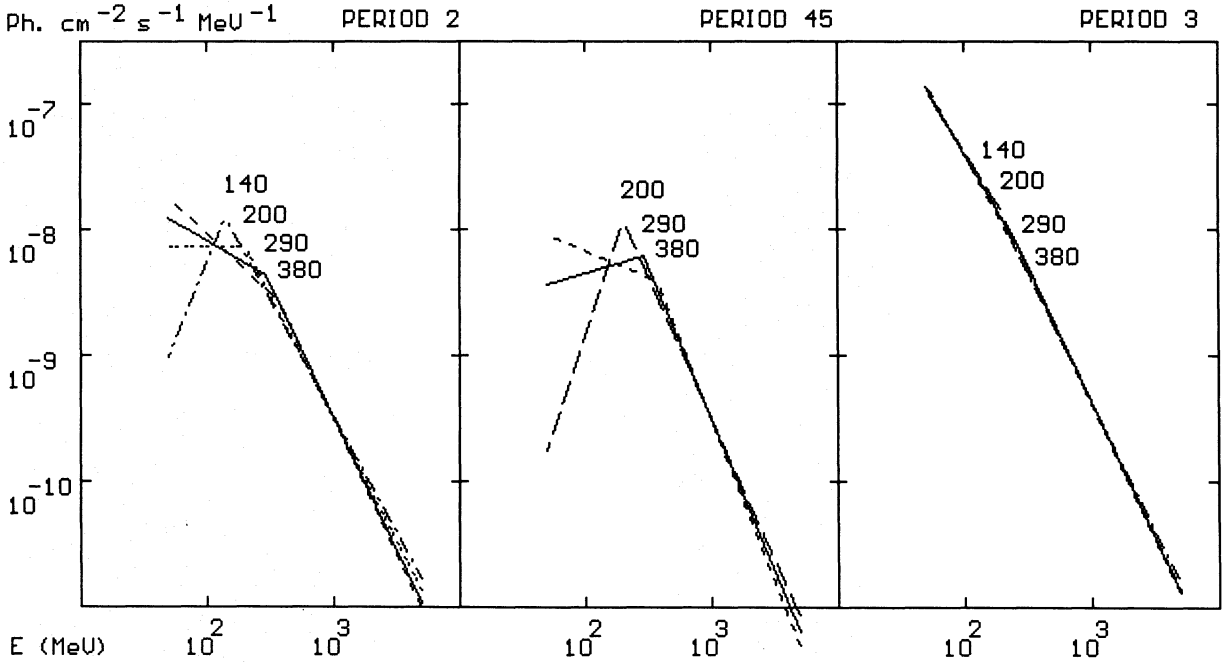

Fig. 4. Maximum-likelihood double-power-law fits to the Vela Interpeak 1 emission, integrated between 0.15 and 0.33 in phase, for observations 2, 45, and 3, respectively, and for different break energies. The $\pm$ 1 σ limits are not displayed to avoid confusion

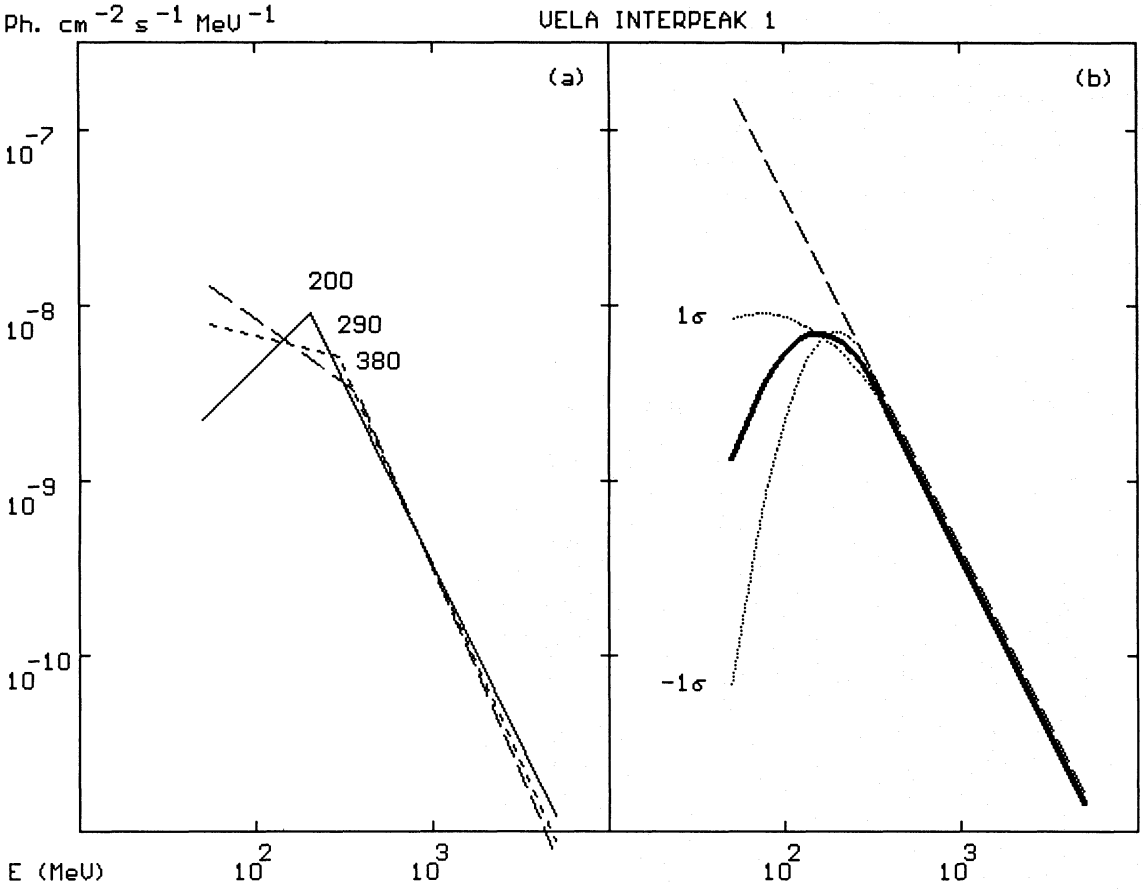

Fig. 5a and b. Maximum-likelihood fit to the Vela Interpeak 1 emission, integrated between 0.15 and 0.33 in phase, in a low state of activity from the combinations of periods 2 and 45: **a** double-power-law fits for break energies at 200, 290, and 380 MeV. Their $\pm$ 1 σ limits are not drawn to avoid confusion. **b** parabolic fit coupled to an E^{-2} spectrum above 380 MeV (thick line) and its $\pm$ 1 σ confidence region (dotted lines). The dashed line shows the high-state spectrum obtained during period 3

Comparing this spectrum to the low-activity average distribution, the likelihood statistics yield a significance of 5.5 σ for a spectral variability. As already mentioned, the stability of the emission from the first peak of the Vela light curve, as well as that of the instrumental and Galactic diffuse emission (see Fig. 2), enables us to rule out an instrumental origin of the variability.

4. Discussion

To summarize our results, in four Geminga observations the $E^{-2.04 \pm 0.08}$ spectrum found at higher energies flattens notably (5 σ) below $\sim$200 MeV while in one observation the spectrum follows a power-law of index -2.02 $\pm$ 0.10 down to 50 MeV. In the same way, the $E^{-2.04 \pm 0.12}$ distribution found for the Vela Interpeak 1 emission at high energy flattens significantly (4 σ) below $\sim$300 MeV in a low state. The high-state spectrum is statistically consistent with a power law of index -2.00 $\pm$ 0.11 from 50 MeV to 5 GeV and the evidence for a slight break at energies lower than 200 MeV is not significant. Therefore, the parallel which was noticed between the Vela and Geminga whole pulsed emissions in the visible, at X rays, and at γ rays is now reinforced with a striking analogy in the γ-ray activity of Geminga and Vela Interpeak 1, both in the spectral distribution of their emission and in its variability. There is a slight difference in the position in energy of the spectral break. It appears towards 100-200 MeV for Geminga and 200-300 MeV for Vela Interpeak 1.

Above a few hundred MeV, the two sources are remarkably stable over the years, in intensity as well as in spectrum. It should further be stressed that this stable high-energy spectrum, of index close to -2.0 $\pm$ 0.1, describes also the γ radiation from the other components of the Vela & Crab light curves in the same energy band (GHC 1988; Clear et al. 1988). The GeV photons are probably produced by the energetic primary particles close to their acceleration site. The different long-term evolutions of the discrete Vela components indicated to GHC distinct origins inside the pulsar magnetosphere. Moreover, the Crab, Vela, and Geminga magnetospheres differ in their extent, hence in the magnetic field strength at various fractional altitudes up to the light-cylinder. Thus, the observation of a common radiation spectrum plausibly reflects similar acceleration mechanisms in different magnetospheres and at different locations inside them. The spectral distributions of synchrotron radiation, for large or small pitch angles, and of curvature radiation all conserve the

power-law spectrum of the radiating particles (Jackson 1962; Epstein 1973). For an observed photon index of $\sim$-2, all three yield an E^{-3} distribution of the number of particles.

The detected variability affects the source emission only below a few hundred MeV; it is largely suppressed for months and enhanced for a few weeks. Estimates of the rise and decay times of 11.4 $\pm$ 1.0 and 137 $\pm$ 39 days, respectively, could be determined for the Vela pulsed emission during one transition (GHC 1988). The Geminga observations are unfortunately too sparse to constrain these parameters. High states do not seem to be rare (1/5 and 2/5 of the observing time for Geminga and Vela), but the low-activity state corresponds to the most common situation, as far as COS-B could determine. One should further remember that intermediate states exist for Vela Interpeak 1. Our dichotomy between low and high states is thus certainly too simplistic. The appearance of a high state two weeks after a giant Vela glitch in 1975 raised the question of a possible relationship between the two events. However, the occurrence of a second high state a few months before another glitch in 1981 did not favour this possibility, nor does the very stable rotation of the Geminga pulsar over 17 years. The combined COS-B and EGRET data (Hermsen et al. 1992; Mattox et al. 1992) do not reveal any glitch activity.

The flattening of the spectrum at lower energies which characterizes the numerous periods of low or intermediate activity provides an explanation for the failure to detect Geminga and Vela Interpeak 1 below 30 MeV with COMPTEL (Strong et al. 1993, Bennett et al. 1993). It also explains the inversion of relative brightness between Crab and Geminga below and above 300 MeV, obvious on the COS-B and EGRET maps of the Galactic anticenter. A preliminary spectrum of Geminga obtained from the EGRET data above 30 MeV is consistent with an intermediate COS-B state and shows a break near 60 MeV (Mayer-Haßelwander et al. 1993).

It is difficult to evaluate the amount of energy implied by the change of state because of the uncertainty both in the source distance and in the solid angle subtended by the radiation beam. In the case of a Vela pulsar at 500 pc, emitting over 2π, the Interpeak 1 luminosity changes by about 10^{34} erg s^{-1} which represents about one hundred times the total power radiated in soft X rays (EINSTEIN: Harnden et al. 1985). In order to scale this number, we observe that the Vela pulsar disposes of 10^{37} erg s^{-1} of spin-down power of which $\sim$1% is converted into γ rays in the MeV-GeV range. The spin-down luminosity of the Geminga pulsar reaches 10^{34} erg s^{-1} for a typical moment of inertia of 1.4-2 10^{45} g cm^2. It lies somewhere within 500 pc of us. With a Vela-like γ-ray efficiency of 1% and a beam filling factor of 2π, the γ-ray flux of $\sim$3 10^{-9} erg cm^{-2} s^{-1} measured in the COS-B range places Geminga at a distance of $\sim$50 pc. So, either Geminga is a very close neutron star or it produces γ rays much more efficiently than does Vela. At 500 pc, its efficiency would reach 90% ! As for Vela, the luminosity variation due to the change of state represents $\sim$180 times the luminosity received in soft X rays (EINSTEIN: Halpern & Tytler 1988; ROSAT: Halpern & Holt 1992). These considerations show that the detected variability is an important event in the γ-ray life of these pulsars. It can affect up to 10% of the total γ-ray luminosity within two weeks.

The similar spectral distributions of the two sources and their comparable evolution with time hints at a common radiation process producing the very hard radiation and a common cause of its variability. The latter may be understood as a suppression/production of soft γ photons or as a variation in energy of an abrupt break in the spectrum of the radiating particles. The first possibility seems unlikely. The detected γ rays are too scarce to suffer from self-absorption at the source. The electron-photon interaction is governed by the Klein-Nishina cross section at these energies. For an optically thick region of radius r in a Vela-type magnetosphere of radius r_c of 4.2 10^8 cm, it requires a particle density of 3 10^{17} $(r/r_c)^{-1}$ cm^{-3}, that is a particle flux at the light cylinder as high as 10^{46} $(\Omega/4\pi)$ $(r/r_c)^{-1}$ sec^{-1}, where the solid angle Ω accounts for the radiation beaming. By contrast, the observed γ-ray flux requires only 2 10^{32} - 4 10^{34} $(\Omega/4\pi)$ particles sec^{-1} through curvature radiation, and 4 10^{33} - 10^{37} $(\Omega/4\pi)$ particles sec^{-1} for synchrotron radiation. Only in the case of small-pitch-angle synchrotron radiation, when some 4 10^{40} - 10^{42} particles sec^{-1} produce the detected γ rays, is the self-absorption limit even remotely approached. From these considerations, it is unlikely that self-absorption explain the observed spectral cut-off, despite its attractive photon index of +1.5 and its natural variability. Pair production on the thermal X rays emitted at the neutron star surface was also calculated to be ineffective. The X-ray flux detected by the EINSTEIN and ROSAT telescopes (Harnden et al. 1985; Halpern & Holt 1992) is not sufficient to absorb 0.1-1 GeV photons inside the magnetosphere because of the small two-photon collision cross section (Lang 1974). Moreover, large variations of the Vela or Geminga X-ray flux have not yet been detected, nor did we find beams of pulsed X rays that could efficiently absorb the γ rays (Halpern & Holt 1992). Magnetic absorption can take place within a few stellar radii from the star surface. But, it cannot account for a time-dependent effect working at low energy. So, for the following discussion, let us adopt a particle distribution which is restricted to energies between $\gamma_1 m_e c^2$ and $\gamma_2 m_e c^2$ (zero elsewhere), and which follows an E^{-3} power law inside this interval.

Optically thin synchrotron radiation with large pitch angles is an appealing process because of its high efficiency and the corresponding short radiation length of the particles. In a 10^6 G field, typical of the Crab outer magnetosphere or of a region half-way to the light-cylinder for Vela or Geminga, the breaks found near 100-200 MeV and 3-6 GeV in the γ-ray spectra of Geminga and Vela Interpeak 1 would correspond to limiting Lorentz factors γ_1 and γ_2 of order 10^5 and 10^6, respectively. Such electron (positron) energies of a few hundred GeV are easily achieved in the current "polar cap"and "outer gap"models of Daugherty & Harding (1982), and of Cheng, Ho & Ruderman (1986). But, because an observer sees a series of very short pulses of radiation, the synchrotron photon spectrum falls only as $E^{-2/3}$ below the lower cut-off energy, which corresponds to the Fourier envelope created by each pulse. This flattening is not fully consistent with the measured spectra in a low state. Below

200 MeV for Vela Interpeak 1 and 140 MeV for Geminga, the likelihood test cannot firmly reject an $E^{-2/3}$ power law (at 2 σ and 2.5 σ, respectively, above the best fit), but it suggests a sharper turn-over of the spectrum.

Optically thin synchrotron radiation with very small pitch angles may be more relevant to these very hard spectra. Because of the wide radiation pattern of the cyclotron emission seen in a frame moving with the particle along the field line, this process gives a photon spectrum, integrated over angles in the observer's frame, that flattens interestingly to E^0 rather than $E^{-2/3}$ below the lower cut-off energy (Epstein 1973). However, compared to larger pitch angles, the radiated power is reduced by approximately $1/\gamma^2$. The sharp turn-over of the low-state spectra implies pitch angles smaller than $1/\gamma_1$, hence a photon spectrum that breaks around $\nu_B.\gamma_1$ and $\nu_B.\gamma_2{}^2/\gamma_1$ (where ν_B is the cyclotron frequency: $eB/2\pi m_e c$). For even smaller pitch angles, less than $1/\gamma_2$, the photon spectrum breaks around $2.\gamma_1.\nu_B$ and $2.\gamma_2.\nu_B$. In any case, to match the observed breaks in a 10^6 G field, this process requires much more energetic particles than before, with Lorentz factors between 10^9 and 10^{11} in excess of what can be reached using the potential drops available in a standard magnetosphere. The radiation reaction limits a particle acceleration to $\sim 10^{13}$ eV (Daugherty & Harding 1982; Cheng, Ho & Ruderman 1986). So, synchrotron radiation with small or very small pitch angles can operate only in the inner magnetosphere where the magnetic field exceeds 10^9 G.

On the other hand, the acceleration the particle feels while loosely gyrating along the field line may be weaker than the acceleration provided by the local curvature of the field line. For a typical radius of curvature of 10^8 cm, curvature radiation dominates over small-pitch-angle synchrotron emission in regions where the field strength drops below 10^9 G. In a typical field of 10^6 G, the observed spectral breaks correspond to particles of energy between 1 and 10 TeV, that is to the most energetic particles produced by a "gap". But, curvature radiation is not efficient. To radiate down to 100 MeV with such a large radius of curvature requires a radiation length comparable to the light-cylinder radius or to a large fraction of it and therefore it is difficult to confine the radiation in phase. Finally, because curvature radiation consists of one short pulse of radiation, its spectral distribution follows the envelope of the periodic synchrotron emission spectrum and falls as $E^{-2/3}$ below the lower cut-off energy. Again, this flattening may not agree with the measured spectra in a low state. New observations with a higher sensitivity and a better energy resolution will be of importance to settle this question. For anyone of the three processes mentioned above, however, the observation of two spectral breaks rather close in energy indicates that the radiating particles are confined to a narrow energy band, covering about one decade.

In the framework of the "polar cap" and "outer gap" models, Harding & Daugherty (1992) and Chiang & Romani (1992) have shown that the γ-ray spectrum produced by photon-pair cascades depends sensitively on aspect angle. Nevertheless, a precession of the pulsar cannot account for the observed variability. It would not leave the high-energy part of the spectrum unchanged and, in the case of Vela, it is ruled out by the simultaneous spectral stability of other components of the light curve. It is noted that for the Crab pulsar the combined results on the Peak2/Peak1 ratio as measured by SAS-2, COS-B, and EGRET suggest a precession or nutation of the neutron star with a period of 14 years. This effect, however, has not been seen at other wavelengths (Thompson et al. 1992). At γ rays, no related change in spectral shape has been noticed so far.

The variability may instead result from a variation of the lower cut-off energy, $\gamma_1 m_e c^2$, of the particle distribution. This would maintain the stability of the high-energy part of the γ-ray spectra. The amplitude of the γ_1 variation depends on the radiative process since the break position in the photon spectrum varies as ${\gamma_1}^{-3}$ for curvature radiation, and as ${\gamma_1}^{-2}$ or ${\gamma_1}^{-1}$ for large or small pitch angle synchrotron emission, respectively. Many effects (such as gap closure, particle radiation length, pair escape from the magnetosphere, cascade development) control the γ_1 boundary and the main cause of its possible instability is not known. For synchrotron emission, a slight displacement of the acceleration site along the field lines, thus changing the cyclotron frequency, may also shift the observed break position.

The induced spectral variability may also apply to the evolution of the main peaks of the Vela pulsed emission. They have been recently seen down to $\sim$1 MeV by COMPTEL (Bennett et al. 1993) and earlier by Tümer et al. (1984) with a different light curve shape and a soft, $E^{-1.6\pm0.2}$, spectrum which connects smoothly to the COS-B or EGRET data. The lack of detection in 1988 by the Figaro experiment (Sacco et al. 1990) reveals a variability similar to that of Interpeak 1. The spectral turn-over, however, occurs at lower energies, around a few MeV, as expected for synchrotron radiation from particles accelerated in a region of weaker magnetic field. Indeed, the 0.42 phase separation of the main peaks implies an origin relatively near to the light-cylinder, while the smaller phase separation of the two broad Interpeak pulses indicates that these come from a region closer to the star. Strickman et al. (1992) reported the detection by OSSE of the Vela main peaks between 60 keV and 550 keV. Their data points smoothly bridge the observations above 1 MeV and the weak detection in ROSAT X-ray data (Ögelman et al. 1991). These observations support the requirement for a break in the γ-ray spectrum of the main peaks.

The detailed study of spectral shapes and time variability as a function of pulsar phase has proved to be of particular importance and should be pursued. The telescopes presently in orbit should facilitate this study and allow a more quantitative comparison with the available pulsar models.

References

Bertsch D.L., et al., 1992, Nat 357, 306
Bennett K., et al., 1993, A&AS january 1993, "Recent advances in high-energy Astrophysics"
Bignami G.F., Caraveo P.A., Paul J.A., 1988, A&A 202, L1
Bignami G.F., Caraveo P.A., 1992, Nat 357, 287
Bloemen J.B.G.M., 1987, ApJ 317, L15
Bloemen J.B.G.M., Reich P., Reich W., Schlickeiser R., 1988, A&A 204, 88

Cheng K.S., Ho C., Ruderman M., 1986, ApJ 300, 522
Chiang J., Romani R.W., 1992, ApJ, in press
Clear J., et al., 1988, A&A 174, 85
Daugherty J.K., Harding A.K., 1982, ApJ 252, 337
Epstein R.I., 1973, ApJ 183, 593
Grenier I.A., Hermsen W., Clear J., 1988, A&A 204, 117 (GHC)
Grenier I.A., Hermsen W., Hote C, 1991, Advances in Space Research 11, n° 8, (8)107
Halpern J.P., Tytler D., 1988, ApJ 330, 201
Halpern J.P., Holt S.S., 1992, Nat 357, 222
Harding A.K., Daugherty J.K., 1992, In: Van Riper K.A. & Ho C. (eds), Proc. of the Los Alamos workshop "Physics of Isolated Pulsars", Taos. Cambridge Univ. Press
Harnden F.R. jr, Grant P.D., Seward F.D., Kahn S.M., 1985, ApJ 299, 828
Hermsen W., et al., 1992, IAU Circ. 5541
Jackson J.D., 1962, Classical Electrodynamics. Wiley, New York
Kniffen D.A., et al., 1992, IAU Circ. 5485
Lang K.R., 1974, Astrophysical Formulae. Springer-Verlag, Berlin
Mattox J.R., et al., 1992, IAU Circ. 5583
Masnou J.L., et al., 1981, Proc. XVIIth Int. Cosmic Ray Conf. 1, 177
Mayer-Haßelwander H.A., 1985, Explanatory supplement to the COS-B Final Database
Mayer-Haßelwander H.A., et al., 1993, A&AS january 1993, "Recent advances in high-energy Astrophysics"
Ögelman H., et al., 1991, Bull. Am. Astron. Soc. 23, 1349.
Sacco B., et al., 1990, ApJ 349, L21
Strickman M., Grove J.E., Matz S., Ulmer M., 1992, IAU Circ. 5557
Strong A.W., et al., 1987, A&AS 67, 283
Strong A.W., et al., 1988, A&A 207, 1
Strong A.W., et al., 1993, A&AS january 1993, "Recent advances in high-energy Astrophysics"
Swanenburg B.N., et al., 1981, ApJ 243, L69
Thompson D.J., et al., 1992, In: Van Riper K.A. & Ho C. (eds), Proc. of the Los Alamos workshop "Physics of Isolated Pulsars", Taos. Cambridge Univ. Press
Tümer O.T., et al., 1984, Nat 310, 214
Wilson R.B., et al., 1992, IAU Circ. 5429

This article was processed by the author using Springer-Verlag TEX A&A macro package 1992.